PERGAMON

International Journal of Heat and Mass Transfer 45 (2002) 1309–1320

International Journal of HEAT and MASS TRANSFER

www.elsevier.com/locate/ijhmt

Wall effect on heat transfer from a micro-cylinder in near-wall shear flow

J.-M. Shi, M. Breuer, F. Durst *

Lehrstuhl für Strömungsmechanik, Universität Erlangen-Nürnberg, Cauerstr. 4, D-91058 Erlangen, Germany

Received 5 December 2000; received in revised form 12 April 2001

Abstract

A two-dimensional numerical study on the heat transfer from small cylinders in near-wall shear flow was carried out taking the conjugated heat conduction in the solid wall into account. The finite volume flow solver (FASTEST-2D) enhanced with multigrid acceleration and the local grid refinement technique was used to achieve efficient computations and accurate numerical results. The effects of the wall thermal conductivity ($10^{-2} \leqslant k_w^* \leqslant 10^4$) on the heat transfer from a cylinder under different flow conditions (the shear parameter $G^* = 0.0033$, 0.01, 0.1 and the cylinder Reynolds number $10^{-3} \leqslant Re_D \leqslant 1.0$) were investigated in detail. The cylinder to wall distance was varied in the range $0.1 \leqslant Y^+ \leqslant 10$ to cover the influence range of the wall effect. It was found that the wall material even of low conductivity, such as mirror glass and Perspex, still has a dominant influence on the heat transfer rate from the cylinder in the vicinity of a wall. However, when Y^+ is above 5.0, the wall effect becomes minor and the average heat loss rate of the cylinder depends only on the cylinder Reynolds number while the shear parameter influences the local Nusselt number distribution. Different heat exchange processes of the fluid and the solid wall were found between materials of high and low conductivities. Based on the numerical results and with the help of dimensional analysis, the physical mechanism of the hot-wire near-wall correction was further revealed.

Keywords: Computational methods; Heat transfer; Measurement techniques

1. Introduction

Heat transfer from a circular cylinder in cross-flow has been intensively investigated. The earlier experimental and analytical results on the effects of a variety of influencing factors have been reviewed by Žukauskas and Žiugžd [1]. Recently, numerical studies have been increasingly focused on this topic. However, most of the available studies are limited to the case where the cylinder is located in a uniform cross-flow. Despite its basic importance in both engineering and science, the problem of a cylinder in shear flows has received relatively little attention. Kwon et al. [2] studied the free shear effect on the flow characteristics over a cylinder for a range of Reynolds numbers from 600 to 1600. Sung et al. [3] investigated the free shear effect on the mass transfer from a cylinder for higher Reynolds numbers of 24,000 and 48,000. They found that the overall mass transfer rate depends almost exclusively on the Reynolds number while the distribution of the local mass transfer rate on the cylinder surface is characterized by the shear rate without a strong dependence on the Reynolds number. Goldstein and Karni [4] examined the effect of a wall boundary layer on the local mass transfer from a cylinder. However, almost no study has dealt with the heat transfer from a cylinder in wall-bounded shear flow except for investigations on the hot-wire near-wall correction. Most of them are experimental, as reviewed by Bruun [5]. The experimental data reflect only the total effect of all possible influencing factors and additionally show a high degree of scatter, which makes it difficult to understand the observed phenomena. Nowadays, numerical analysis is a powerful tool for overcoming this

* Corresponding author. Tel.: +49-9131-852-9500; fax: +49-9131-852-9503.

E-mail addresses: shi@lstm.uni-erlangen.de (J.-M. Shi), breuer@lstm.uni-erlangen.de (M. Breuer), durst@lstm.uni-erlangen.de (F. Durst).

0017-9310/02/$ - see front matter
PII: S0017-9310(01)00225-3

Nomenclature

c_p	specific heat at constant pressure
C_U	velocity correction factor
D	cylinder diameter
Ec	Eckert number
g	gravitational acceleration
G	shear rate
Gr	Grashof number
H	thickness of the solid wall
k	thermal conductivity
Nu	Nusselt number
P	pressure
Pr	Prandtl number
Re	Reynolds number
Re_D	cylinder Reynolds number
T	temperature
U_τ	friction velocity
U, V	Cartesian velocity components
x, y	Cartesian coordinates
Y	cylinder to wall distance

Greek symbols

α	heat diffusion coefficient
β	volumetric thermal coefficient expansion
μ	dynamic viscosity
ν	kinematic viscosity
ρ	fluid density
τ	temperature loading
τ_w	wall shear stress
Φ	viscous dissipation function

Indices

0	actual value
c	characteristic quantities
D	at the cylinder location
∞	free-stream
f	flow region
num	numerical value
w	solid wall
W	at the cylinder surface
$*$	non-dimensional quantity
$+$	in wall units

experimental disadvantage. The few published numerical studies were made by Bhatia et al. [6], Chew et al. [7] and Lange et al. [8] and contradicted each other and also the experimental data in cases of walls of low conductivity. As a result, some confusion regarding the heat transfer behavior of a hot-wire in shear flow close to poorly conducting walls remained for many years. The problem was successfully solved by a recent numerical investigation by Durst et al. [9], who for the first time took the conjugated heat conduction in the solid wall into account. Actually, all these studies were specific for hot-wire wall corrections, and the effects of wall thermal conductivity, shear rate ($G = \partial U/\partial y = U_D/Y$) and Reynolds number on the characteristics of the local heat transfer of a cylinder in a near-wall shear flow were not studied. The heat exchange between the fluid and the solid wall was also not analyzed.

Knowledge of these effects and detailed information on the local heat transfer rate at the cylinder surface and on the heat exchange between the fluid and the solid wall are useful not only for hot-wire near-wall measurements but also for precise micro-machinery designs. In such flow situations, the cylinder Reynolds number is typically in the creeping range, so no flow separation occurs around the cylinder. In addition, the flow and heat transfer remain steady. Despite this simplicity, the overall problem is still complex. The cylinder is generally of micrometer size and may be only a few diameters away from the wall. As a result, the convective heat transfer of the cylinder will depend significantly on the coupled heat conduction in the solid wall, as was confirmed by Durst et al. [9] and relatedly by Lacroix and Joyeux [10]. Therefore, it is of interest not only to understand under what conditions the cylinder will become subject to the influence of wall conduction, but also further to examine how this influence will affect the heat transfer characteristics from the cylinder under different flow conditions ($Re_D = U_D \cdot D/\nu_\infty$ and G) and to understand how the flow region and the solid wall are coupled.

In the present work, a heated cylinder in a linear wall shear flow of cylinder Reynolds number ranging from 10^{-3} to 1.0 was investigated numerically. The physical model for this problem is described in Section 2. Considering that the numerical grid and the local resolution in the region close to the cylinder are the key points to guarantee numerical accuracy, a well tested local-block refinement algorithm [11] was used. The numerical details are provided in Section 3. The Reynolds number was systematically varied to obtain a non-dimensional distance $Y^+ = YU_\tau/\nu$ increasing from 0.1 to 10 to cover the influence range of the wall conduction. Wall materials of both low and high conductivities under different flow conditions (Re_D and G) were investigated. Detailed information was obtained for the local heat transfer rate from the cylinder. The effects of wall conductivity, shear rate and Reynolds number are discussed in Section 4. The interaction between the "temperature influence region" of a hot-wire and the solid wall and the heat exchange between the fluid and the wall material were analyzed. This leads to a better understanding of the physical mechanism for the required hot-wire velocity

correction close to different wall materials under different flow conditions.

2. Physical model and boundary conditions

A two-dimensional steady laminar problem including conjugated heat transfer in the solid wall was considered. The physical model for the present problem is illustrated schematically in Fig. 1. An infinite circular cylinder of diameter $D = 5$ μm and temperature $T_W = 100$ °C was mounted in a linear wall-bounded shear flow. The fluid considered was air at an inflow (ambient) temperature of $T_\infty = 20$ °C. The cylinder to wall distance was in the range $10 \leqslant (Y/D) \leqslant 300$. For each distance, several shear rates G were applied, based on which the friction velocity varied in the range $0.006 \leqslant U_\tau \leqslant 0.307$ m/s. The Reynolds numbers Re_D based on the cylinder diameter D and the inflow velocity U_D at the height of the cylinder location are in the range 10^{-3}–1.0. The resulting non-dimensional wall distances ($Y^+ = [Y U_\tau]/\nu$) cover a range from 0.1 to 10. The thickness of the plate is $H = 300D$ or 1.5 mm. Materials of different thermal conductivities (aluminum, $k_w^* = k_w/k_\infty = 9186$; glass, $k_w^* = 29.6$; Perspex, $k_w^* = 7.2$; air, $k_w^* = 1.0$ and two artificial materials with $k_w^* = 0.1$ and 0.01) were investigated. The plate is adiabatic at the bottom surface while the heat conduction in the plate is coupled to the flow region by means of temperature continuity and heat flux conservation at the interface (top surface). Both lateral ends of the plate were set to take a constant ambient temperature. No-slip flow conditions, i.e., $U = 0$ and $V = 0$, were defined on all wall boundaries. The flow on the upper boundary of the integration domain was assumed to be undisturbed and a zero gradient boundary condition for a fully developed flow was assigned at the outflow boundary. As indicated in Fig. 1, the computational domain in the y-direction was accordingly extended between $1000D$ and $3000D$ (more than 20 wall units) from the wall based on extensive numerical tests. A domain size of not less than $6000D$ upstream and $10000D$ downstream of the cylinder were chosen to eliminate the influence of the boundary conditions.

3. Numerical details

3.1. Mathematical model

For steady flow and heat transfer around a two-dimensional cylinder, the non-dimensional governing equations expressing the conservation of mass, momentum and energy for an incompressible fluid with temperature-dependent fluid properties are, in Cartesian coordinates, as follows:

$$\frac{\partial(\rho^* U_i^*)}{\partial x_i^*} = 0, \tag{1}$$

$$\frac{\partial(\rho^* U_i^* U_j^*)}{\partial x_i^*} = -\frac{\partial P^*}{\partial x_j^*} + \frac{1}{Re}\frac{\partial}{\partial x_i^*}\left[\mu^*\left(\frac{\partial U_j^*}{\partial x_i^*} + \frac{\partial U_i^*}{\partial x_j^*}\right)\right] + \frac{Gr}{Re^2} T^*, \tag{2}$$

$$c_p^* \frac{\partial(\rho^* U_i^* T^*)}{\partial x_i^*} = \frac{1}{Re\,Pr}\frac{\partial}{\partial x_i^*}\left(k^* \frac{\partial T^*}{\partial x_i^*}\right) + \frac{Ec}{Re}\Phi^*, \tag{3}$$

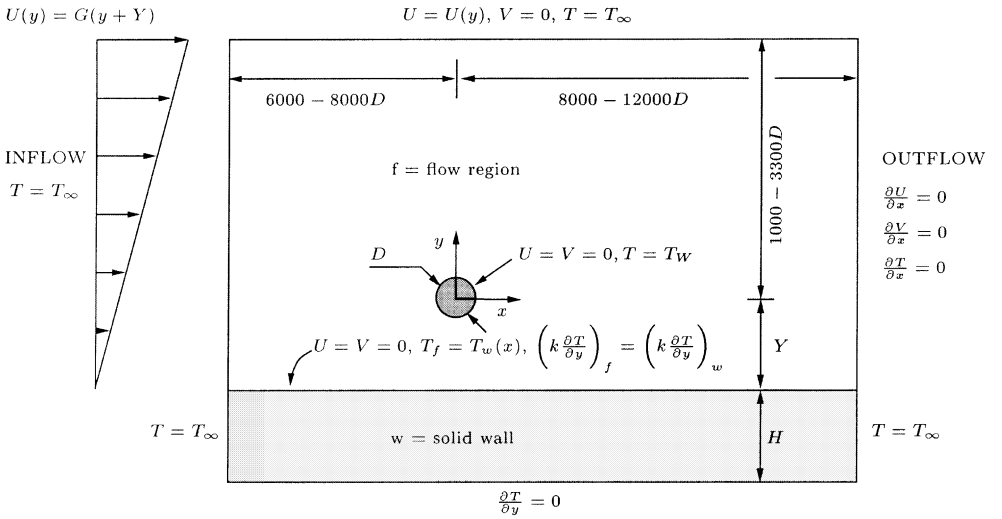

Fig. 1. Schematic diagram of the physical model for a heated cylinder in a near-wall shear flow.

where $i, j = 1, 2$ and Φ^* is the normalized viscous dissipation function, given by

$$\Phi^* = \mu^* \left(\frac{\partial U_i^*}{\partial x_j^*} + \frac{\partial U_j^*}{\partial x_i^*} \right) \frac{\partial U_i^*}{\partial x_j^*}. \quad (4)$$

Considering the characteristics of the wall-bounded shear flow, the velocity components and coordinates are normalized by the friction velocity $U_c = U_\tau = \sqrt{\tau_w/\rho_\infty}$ and the molecular diffusion length $l_c = \nu_\infty/U_\tau$, respectively. ρ^*, μ^*, k^* and c_p^* are dimensionless properties (density, viscosity, thermal conductivity and specific heat at constant pressure, respectively) normalized by the corresponding values at the inflow temperature T_∞. $T^* = (T - T_\infty)/(T_W - T_\infty)$ is the dimensionless temperature normalised by $T_W - T_\infty$. The non-dimensional parameters appearing in the governing equations are as follows:

$$\text{Eckert number}: \ Ec = \frac{U_c^2}{c_{p\infty}(T_W - T_\infty)},$$

$$\text{Grashof number}: \ Gr = \frac{l_c^3 g \beta \rho_\infty^2 (T_W - T_\infty)}{\mu_\infty^2},$$

$$\text{Prandtl number}: \ Pr = \frac{\mu_\infty c_{p\infty}}{k_\infty},$$

$$\text{Reynolds number}: \ Re = \frac{U_c l_c}{\nu_\infty} = 1,$$

where g is the gravitational acceleration, β the coefficient of volumetric thermal expansion.

Applied to the heat conduction in the solid wall, the simplified energy equation reduces to a Laplacian equation. Thus only the dimensionless thermal conductivity of the wall material k_w^* and the wall thickness H/D remain as relevant parameters.

In the present study, the temperature dependence of the transport properties of the fluid were taken into account. ρ^*, μ^*, k^* and c_p^* are treated as quadratic polynomial functions of T^*, whose coefficients are interpolated based on the VDI-Wärmeatlas [12]. The investigations were restricted to cases where continuum and incompressibility of the fluid can be assumed. Natural convection and viscous dissipation effects are small owing to the dimensions and temperatures involved in the present investigation. Therefore, the last terms in Eqs. (2) and (3) were neglected (see, e.g. [13,14]).

3.2. Numerical method and computational grids

For the spatial discretization of Eqs. (1)–(3), a finite volume method with a colocated arrangement of the variables was employed, as described by Demirdžić and Perić [15]. The convection and diffusion contributions to the fluxes were evaluated using a central differencing scheme. In order to ensure mass conservation, a pressure-correction equation was solved following the SIMPLE algorithm proposed by Patankar and Spalding [16]. Details of the discretization and the pressure–velocity coupling can be found elsewhere [15,17]. A nonlinear multigrid scheme was employed for convergence acceleration (see, e.g. [18]). Convergence was assumed to be satisfied when the maximum sum of the normalized absolute residuals in all equations was reduced by six orders of magnitude.

In order to improve the accuracy of the numerical results without a decrease in efficiency and to optimize the utilization of the available computational resources, a local grid refinement technique was employed. For the local refinement procedure, the computational domain was divided into blocks and each block was discretized with a different mesh density to retain a structured grid [11,13,14]. More than 500 grid points were applied on the finest grid level at the cylinder surface to ensure a high accuracy of the results. In total, about 10^5 grid points on the fifth multigrid level were used in the computations. As an example, a zoomed view of the grid and the core region on the third multigrid level for one case of $Y/D = 100$ are shown in Fig. 2.

The numerical code was verified by extensive predictions of the flow and heat transfer around a heated two-dimensional cylinder under free-stream conditions in the Re_D range 10^{-4}–10^2 [13,14] and the recent successful studies of hot-wire near-wall corrections [8,9]. The combination of high efficiency with high accuracy provided by the local-block refinement is essential to the realization of this investigation.

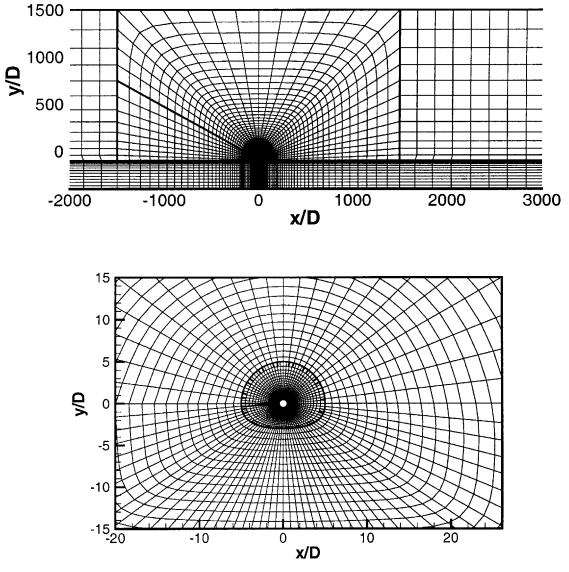

Fig. 2. Example of computational grid ($Y/D = 100$) and zoom of the locally refined region (both at the third of a total of five multigrid levels).

4. Results and discussion

4.1. Definitions and analysis

In order to describe the local heat transfer rate of the cylinder, the local Nusselt number distribution $Nu(x)$ on the cylinder surface is introduced. The definition is

$$Nu(x) = \frac{(\partial[T(x) - T_\infty]/\partial r)|_W}{(T_W - T_\infty)/D}, \tag{5}$$

where r is the radial component of a cylindrical coordinate system with the same origin as the Cartesian coordinate system as sketched in Fig. 1 and x is the x-component of the Cartesian coordinate system. The subscript W denotes the cylinder surface where $r = \sqrt{x^2 + y^2} = D/2$ is satisfied. According to the definition of the dimensionless quantities in Section 3, Eq. (5) can be rewritten as

$$Nu\left(\frac{x}{D}\right) = -\left.\frac{\partial T^*(x/D)}{\partial(r/D)}\right|_W. \tag{6}$$

The mean Nusselt number Nu can be averaged from $Nu(x/D)$ over the cylinder surface.

Without considering the heat conduction in the solid wall, the relevant quantities to formulate the flow and heat transfer in the flow region are U_D, Y, D, T_W, T_∞, c_p, k, ρ, μ, β and g. For a steady-state coupling with the solid wall, only the dimensionless thermal conductivity of the wall material k_w^* and the wall thickness H/D remain as additional relevant parameters (see Section 3). Therefore, a dimensional analysis yields the following general dependence of Nu on the parameters

$$Nu = f\left(Re_D, \frac{Y}{D}, \frac{T_W}{T_\infty}, Pr, Gr, Ec, k_w^*, H/D\right). \tag{7}$$

As mentioned in Section 3, the influence of free convection and viscous heating is minor under the flow conditions considered here, hence the dependence on Gr and Ec can be neglected. Therefore, Eq. (7) is simplified

$$Nu = f\left(Re_D, \frac{Y}{D}, \frac{T_W}{T_\infty}, Pr, k_w^*, H/D\right), \tag{8}$$

where the shear effect ($G = \partial U/\partial y = U_D/Y$) is implicitly included. For an explicit analysis, we introduce the convection and diffusion time-scales:

$$t_{conv} = \frac{D}{U_D}, \quad t_{diff} = \frac{D^2}{v}.$$

Hence two non-dimensional shear parameters can be defined:

$$G_1^* = G,\ t_{conv} = \frac{U_D}{Y}\frac{D}{U_D} = \left(\frac{Y}{D}\right)^{-1}, \tag{9}$$

$$G_2^* = G,\ t_{diff} = \frac{U_D}{Y}\frac{D^2}{v} = Re_D\left(\frac{Y}{D}\right)^{-1}. \tag{10}$$

If a dimensionless diameter defined as $D^+ = DU_\tau/v$ is introduced, then combinations of Re_D and Y/D yield the following relationships:

$$Re_D\frac{Y}{D} = Y^{+2}, \quad Re_D\left(\frac{Y}{D}\right)^{-1} = G_2^* = D^{+2}.$$

And obviously we have

$$Re_D = \frac{t_{diff}}{t_{conv}} = Y^+D^+.$$

Based on the above analysis, it is clear that the influence of the cylinder diameter D^+ on the heat transfer often mentioned in the literature on hot-wire near-wall correction is equivalent to the shear effect G_2^*. Physically, it reflects the ratio of the diffusion time t_{diff} to the time of convection needed from the cylinder to the wall Y/U_D. Additionally, the analysis indicates that any pair of these dimensionless parameters ($Re_D, Y/D, G_1^*, G_2^*, Y^+$ and D^+) is suitable for characterizing the flow condition. Therefore, a useful expression can be obtained for the hot-wire near-wall measurement

$$Nu = f\left(Y^+, D^+, \frac{T_W}{T_\infty}, Pr, k_w^*, H/D\right). \tag{11}$$

In the present study, $Pr \approx 0.72$, $T_W\ [K]/T_\infty\ [K] = 1.27$ and $H/D = 300$ were not varied. We concentrate on the influence of k_w^* in combination with that of the flow condition parameters. First, the k_w^* effect on the local heat transfer rate of a cylinder at different Y^+ will be discussed in detail in Section 4.2. In the subsequent subsection, the shear effect G_2^*, i.e., the influence of D^+ and Re_D in the range beyond the wall effect, will be studied. Finally, we apply the obtained results to the hot-wire near-wall correction and discuss the physical mechanism.

4.2. Effect of wall thermal conductivity

To make a detailed examination of the wall effect on the heat transfer characteristics of a cylinder, the local Nusselt number distributions $Nu(x/D)$ on the cylinder surface are displayed in this section for different wall materials and different cylinder to wall distances. In all figures, the lower side surface facing to the wall is distinguished from the upper side by broken lines. First, we check the influence of the wall thermal conductivity (Fig. 3) in the case of a cylinder located at a very small distance from the wall ($Y^+ = 0.2$, resulting from $Re_D = 0.004$ and $G_1^* = 0.1$), where the wall effect is expected to be very strong. The result for a cylinder in a uniform free flow with the same Reynolds number [19] is also displayed for comparison. Despite the same flow condition,

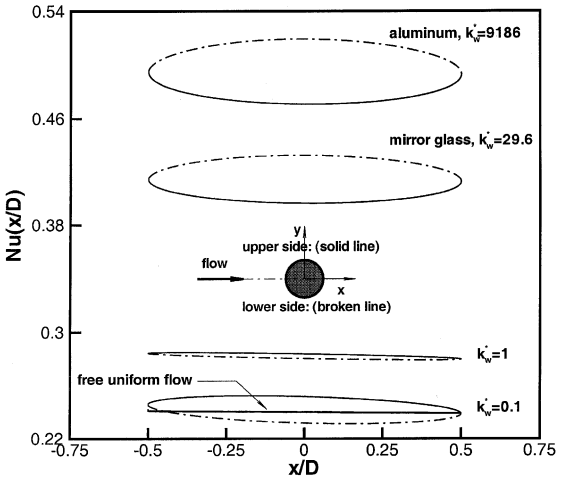

Fig. 3. Local Nusselt number $Nu(x/D)$ of a cylinder at $Y^+ = 0.2$ ($Re_D = 0.004$ and $G_1^* = 0.1$) from walls of different conductivities.

distinct $Nu(x/D)$ distributions can be observed in Fig. 3 corresponding to walls of different thermal conductivities. The heat loss from the cylinder is significantly enhanced both in case of a wall of aluminum ($k_w^* = 9186$) and a wall of mirror glass ($k_w^* = 29.6$). Moreover, the local heat transfer rate on the lower side of the cylinder is found to surpass that on the upper side for both wall materials. That indicates that the wall conduction effect is still significant when a cylinder is located in the proximity of poorly conducting walls (e.g., mirror glass, $k_w^* = 29.6$). On the other hand, the heat transfer rate on the lower side of the cylinder is smaller than that on the upper side in cases of artificial walls $k_w^* \leqslant 1$). The difference in the heat transfer rate between the upper and lower side of the cylinder increases with decreasing thermal conductivity of the wall material. This again shows the important effect of the wall thermal conductivity. However, it is interesting that the heat loss rate of the cylinder for $k_w^* = 1$ (a wall with the same conductivity as the fluid) is predicted to be much higher than that in the free stream case. This phenomenon is difficult to understand if we exclude the influence of the flow distortion due to the presence of a wall close to a cylinder. A further investigation on this effect is on-going.

The above results are very useful for clarifying the existing confusion on the physical cause of the heat transfer modification from a hot-wire in the vicinity of walls of low conductivity (e.g., mirror glass). Chew et al. [7] suggested the flow distortion due to the presence of a wall as the main reason whereas Lange et al. [8] proposed wall conduction. The present results for mirror glass provide explicit evidence for the latter interpretation; however, the role of the flow distortion might not be minor according to the results for walls of $k_w^* = 1$.

The overshoot of $Nu(x/D)$ on the lower side decreases with increasing Y^+, reflecting a decreasing influence of the wall conduction, as shown in Fig. 4 for an aluminum wall ($k_w^* = 9186$) and a mirror glass wall ($k_w^* = 29.6$) for comparison. In the case of a mirror glass wall, the overshoot reduces to zero at $Y^+ = 1.4$ (not shown here) and a larger heat loss $Nu(x/D)$ occurs on the upper side of the cylinder as Y^+ increases further. In comparison, the influence of an aluminum wall is obviously stronger than that of a mirror glass wall under the same flow conditions. Hence the turning point of the overshoot is expected to be at a larger distance $Y^+ \approx 1.9$ (not shown here). The wall effect becomes negligible at $Y^+ \approx O(10)$

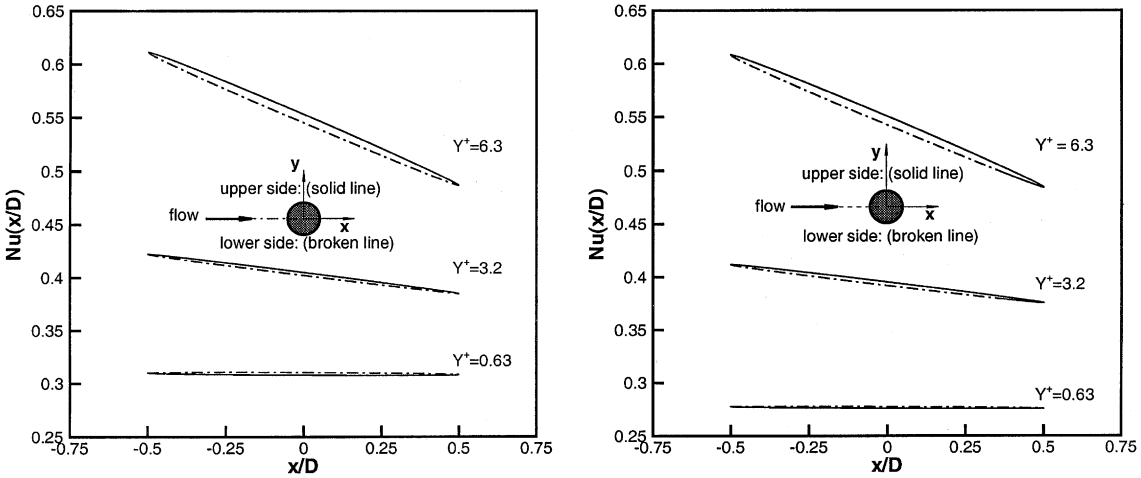

Fig. 4. Influence of an aluminum wall ($k_w^* = 9186$, left) and a glass wall ($k_w^* = 29.6$, right) on the local Nusselt number $Nu(x/D)$ of a cylinder close to these walls.

for all materials, e.g., a maximum difference in $Nu(x/D)$ of less than 1% is found between the case of an aluminum wall and a mirror glass wall at $Y^+ = 6.3$. For both cases, the averaged $Nu(x/D)$ value of both sides of the cylinder is almost the same as the free-stream case. This indicates a negligible effect of wall conduction.

The dependence of the heat loss rate of the cylinder on the thermal conductivity of the wall material k_w^* and the cylinder-wall distance Y^+ can be well understood by checking the field information of temperature isolines around the cylinder and in the solid materials. Figs. 5 and 6 display the temperature distributions for the case of an aluminum and a mirror glass wall for $Y^+ = 0.63$ and $Y^+ = 10$, respectively. As shown in Fig. 5, the temperature distribution in the region of interest is strongly influenced by the heat conduction in the solid wall when $Y^+ = 0.63$. Furthermore, much higher temperature gradients are caused around the cylinder by the higher conductivity of an aluminum wall compared with a mirror glass wall. In comparison, the temperature distributions around the cylinder at $Y^+ = 10$ are found to be similar for the two wall materials (Fig. 6).

4.3. Influence of Reynolds number and shear rate

According to the analysis in Section 4.1, the heat transfer of a cylinder in this investigation depends on two additional flow parameters, Re_D and the shear parameter G_1^* or G_2^*. In order to display the Reynolds number effect on the local heat transfer rate from the cylinder, the $Nu(x/D)$ distributions for the case of a constant shear parameter ($G_1^* = 0.01$) and an aluminum wall with various Re_D are presented in Fig. 7, together with the corresponding results for a cylinder in a free uniform flow ($G_1^* = 0$) from Lange [19] for comparison. Without considering the natural convection effect, the flow and heat transfer in the free-stream case are symmetrical with respect to the x-axis at such small values of Re_D as considered here. Hence the values of $Nu(x/D)$ on the upper side of the cylinder are expected to coincide with those on the lower side. Moreover, a linear distribution, $Nu(x/D) = Nu(Re_D) - a(Re_D) \cdot (x/D)$, is found in Fig. 7 (right). Here, $Nu(Re_D)$ is the average value and $a(Re_D)$ is the gradient with respect to x/D. Owing to the effect of the shear rate and the wall conduction, the problem becomes nonsymmetrical and, as a result, a "elliptic"-shaped $Nu(x/D)$ distribution is found for the case of a cylinder close to an aluminum wall (Fig. 7, left). However, the "long-axis" of the ellipse is almost parallel to the linear distribution in the free-stream case for the same value of $Re_D a(Re_D)$. $a(Re_D) \approx 0$ is observed for $Re_D = 0.004$. This indicates that the diffusive heat transfer is dominant in cases of very low Reynolds numbers. The

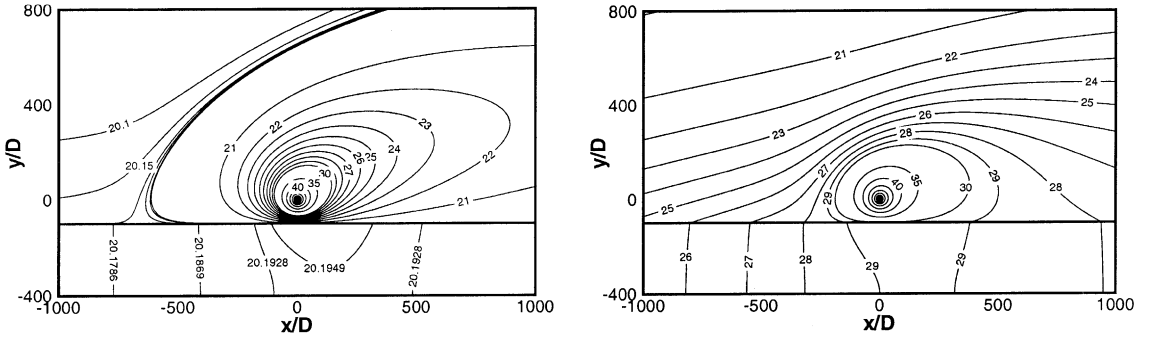

Fig. 5. Temperature isolines (°C) around the cylinder and in the wall at $Y^+ = 0.63$ resulting from $Re_D = 0.004$, $Y/D = 100$. Case (a): an aluminum wall, $k_w^* = 9186$ (left). Case (b): a mirror glass wall, $k_w^* = 29.6$ (right).

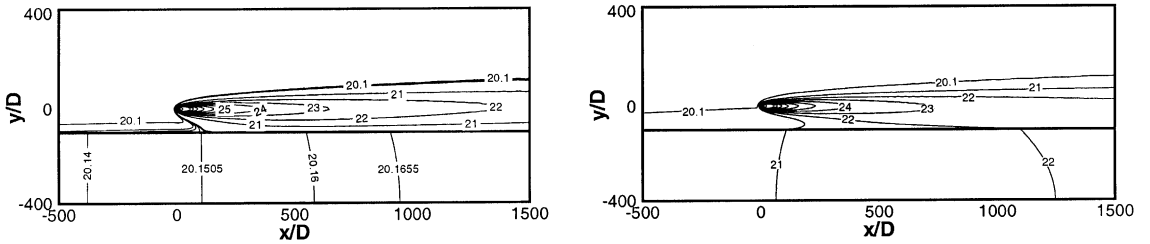

Fig. 6. Temperature isolines (°C) around the cylinder and in the wall at $Y^+ = 10$ resulting from $Re_D = 1$, $Y/D = 100$. Case (a): an aluminum wall, $k_w^* = 9186$ (left). Case (b): a mirror glass wall, $k_w^* = 29.6$ (right).

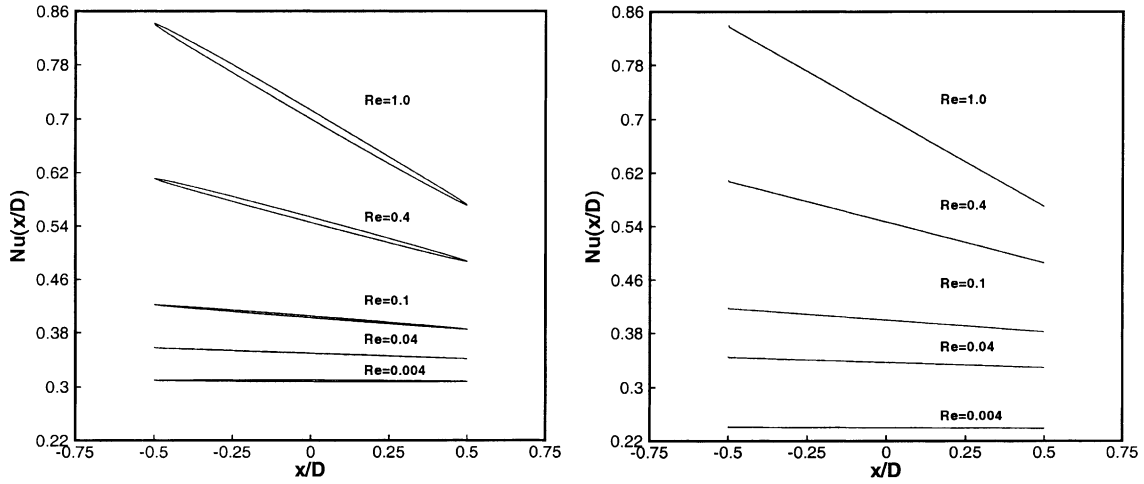

Fig. 7. Influence of the Reynolds number Re_D on the local Nusselt number $Nu(x/D)$ of a cylinder in shear flow close to an aluminum wall ($k_w^* = 9186$) at $G_1^* = 0.01$ (left) and in free uniform flow from [19] (right).

gradient a increases with increasing Re_D, which physically reflects an increased contribution from the convective heat transfer.

The long-axis of the $Nu(x/D)$ ellipse represents the average values of the upper and lower sides. A careful examination of Fig. 7 shows that the linear $Nu(x/D)$ distribution in uniform flow ($G_1^* = 0$) coincides with the corresponding long-axis ($G_1^* = 0.01$) at $Y^+ = 6.3$ ($Y/D = 100$, $Re_D = 0.4$) and $Y^+ = 10$ ($Y/D = 100$, $Re_D = 1$), where the influence of the wall effect is negligible. This suggests that, similar to the case of a uniform flow, the average heat loss rate Nu of a cylinder in a shear flow and the gradient a of its distribution are principally determined by the cylinder Reynolds number Re_D, and the effect of the shear rate (G_1^* or G_2^*) is minor.

However, the heat transfer difference between the upper and lower sides of a cylinder,

$$\Delta Nu\left(\frac{x}{D}\right)\Big/Nu = \left[Nu\left(\frac{x}{D}\right)_{\text{upper}} - Nu\left(\frac{x}{D}\right)_{\text{lower}}\right]\Big/Nu$$

is mainly characterized by the shear rate, as demonstrated in Fig. 8 for three cases beyond the influence range of the wall conduction. As can be expected, $\Delta Nu(x/D)/Nu$ increases with increasing G_1^* or G_2^* at the same Reynolds number. However, it is worth noting that with the same value of $G_1^* = 0.01$, the case with a larger value of $G_2^* = Re_D{\cdot}G_1^*$ corresponds to a higher $\Delta Nu(x/D)/Nu$. Therefore, the relative heat transfer difference between the upper and lower sides of a cylinder is better characterized by the shear parameter G_2^*. The reason is that $G_1^* = D/Y$ contains only the geometric configuration whereas the flow information Re_D is already included in G_2^*.

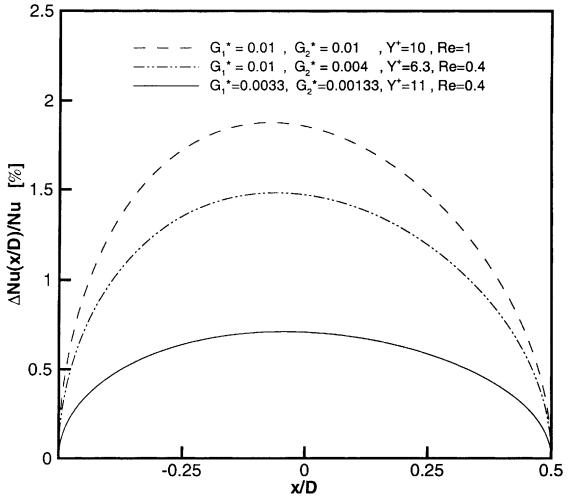

Fig. 8. Shear effect on the local Nusselt number of a cylinder, $\Delta Nu(x/D)/Nu = [Nu(x/D)_{\text{upper}} - Nu(x/D)_{\text{lower}}]/Nu$.

4.4. Implications for hot-wire near-wall correction

It is clear that a hot-wire measures a larger apparent velocity U_{appa} than the real value U_0 when it is applied to flow fields close to highly conducting walls, e.g., aluminum. Hence a positive velocity correction $\Delta U = (U_{\text{appa}} - U_0)$ is needed. In this case, a general understanding of the mechanism was reached based on the available literature. The numerical results of the authors [9] for an aluminum wall ($k_w^* = 9186$) and of Lange et al. [8] for a perfectly conducting wall ($k_w^* = \infty$) were found to agree well with the experimental data in the literature.

However, as mentioned above, contradictory results (small positive correction, no correction and negative correction) and different understandings [7,8] exist in the literature for poorly conducting wall materials such as mirror glass or Perspex. Based on the present study, the physical problem is better understood. For convenience of the explanation, we display again the part of the numerically predicted hot-wire velocity corrections close to poorly conducting walls (mirror glass, $k_w^* = 29.6$, and Perspex, $k_w^* = 7.2$) in Fig. 9. The complete numerical correction results including cases of highly conducting walls and artificial walls ($k_w^* < 1$) can be found in Durst et al. [9].

The results in Fig. 9 are presented in the form of the correction factor $C_U = U_0/U_{appa}$. Under this definition, a positive velocity correction observed in cases of highly conducting walls corresponds to $C_U < 1$. Region (b) of Fig. 9, where $C_U > 1$ ($\Delta U < 0$, negative correction needed) is observed, is worth special noting. This phenomenon was predicted for the first time by Lange et al. [8] with an adiabatic wall ($k_w^* = 0$) (included in Fig. 9), but it is not clear whether this phenomenon occur in the cases of realistic wall materials. In fact, it can also be recognized in the experimental data of Ligrani and Bradshaw [20] with a mirror glass wall and Chew et al. [21] with a Plexiglas wall, as shown in Fig. 9. Based on the detailed numerical results in Sections 4.2 and 4.3, the effect of heat conduction in the solid wall on the hot-wire measurement under different flow conditions and close to different wall materials can be better understood. With the help of further analysis in the following section, the present predicted negative velocity correction $C_U > 1$ for poorly conducting materials can be confirmed and the physical mechanism of the different velocity corrections required for hot-wire measurements corresponding to different situations can be revealed.

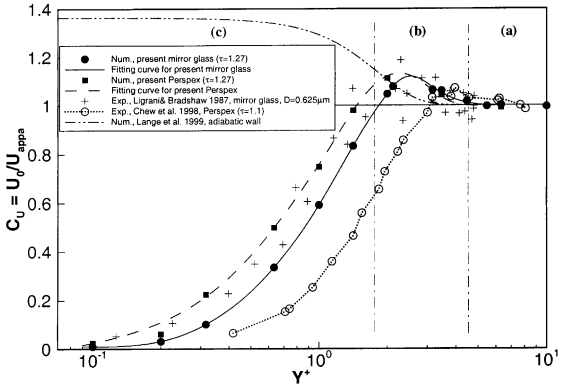

Fig. 9. Comparison of numerical and experimental values of the velocity correction factor C_U in cases of walls of low conductivity (mirror glass, Perspex).

4.5. A physical explanation of hot-wire near-wall corrections

The field information on temperature isolines at different Y^+ (Figs. 5 and 6) clearly suggests the important influence of the interaction of the temperature influence region of a hot-wire and the wall (Fig. 10) and of the heat exchange process between the fluid and the solid wall on the heat loss rate from a wire. First, we make a simplified dimensional analysis to explain idea of the temperature influence region of a wire. Assuming that the heat transfer around a hot-wire in a free uniform flow can be described by two independent processes, diffusion (see Eq. (14)) and uniform convection, we have the following relationships:

$$\text{diffusion}: \quad x^2 + y^2 = l_c^2,$$
$$\text{convection}: \quad x_0 = x + U_\infty t_c, \quad y_0 = y,$$

where $t_c = l_c^2/\alpha_c$ as defined in Eq. (16) and l_c, t_c are the characteristic length and time of the diffusion process, respectively. A combination of the two processes together with a simple derivation yields a parabolic expression for the "temperature influence region" of the wire

$$\frac{x_0}{D} + \frac{1}{4PrRe_D}\left(\frac{y_0}{D}\right)^2. \tag{12}$$

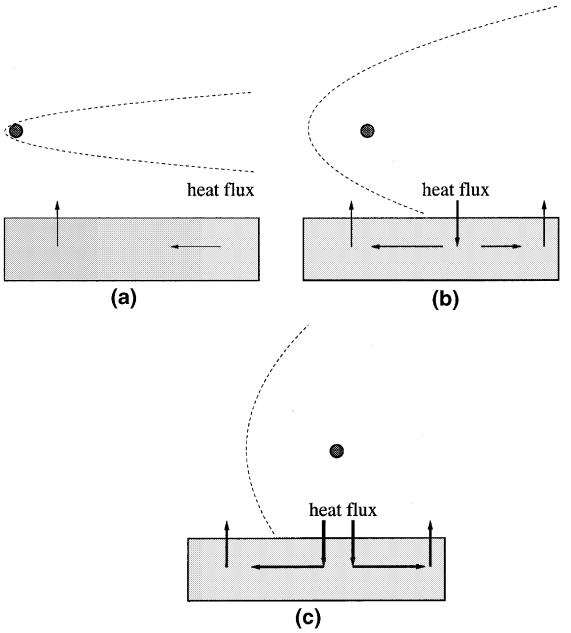

Fig. 10. Schematic temperature influence region of a hot-wire and the heat exchange process between the fluid and the solid wall at various wire to wall distance Y^+: (a) $C_U = 1.0$; (b) $C_U > 1.0$; (c) $C_U < 1.0$.

Applying Eq. (12) to the hot-wire near-wall measurement and neglecting the shear effect, we obtain the intersection point $(X/D, Y/D)$ of the parabolic curve with the fluid–wall interface

$$\frac{X}{D} = Pr\frac{Y}{D}(Y^+)^2 - \frac{1}{4Pr\,Re_D}. \tag{13}$$

Considering the relationship $Y^{+2} = Re_D \cdot (Y/D)$ obtained in Section 4.1, we obtain from Eq. (13) that for a fixed Y/D, the intersecting location (X/D) moves in the downstream direction as Re_D (or Y^+) increases.

The above analysis is simplified because the shear effect and the coupled heat conduction in the solid wall have not been taken into account. However, this simplification is sufficient to give us a qualitative idea of the interaction between the "temperature influence region" and the solid wall, which is one of the essential parts of the mechanism responsible for the different velocity correction values required for a hot-wire corresponding to different wire-to-wall distances Y^+.

The numerical results for the heat exchange between the fluid and the solid wall at the interface $k^*(\partial T/\partial y)$ are displayed in Fig. 11 for the cases of an aluminum wall $(k_w^* = 9186)$ and a mirror glass wall $(k_w^* = 29.6)$ for various values of Y^+. According to the definition, positive values mean the heat flux from the fluid into the solid wall and negative fluxes are the heat fed back into the fluid from the solid wall. The heat feedback in the case of an aluminum wall is observed to be very weak for all Y^+ whereas significant heat flux fed back into the fluid is found from a mirror glass wall. The influence of the material properties on the heat feedback can be understood by a dimensional analysis of the simplified unsteady heat conduction equation in the solid wall

$$\rho c_p \frac{\partial T}{\partial t} = \frac{\partial(k(\partial T/\partial x_i))}{\partial x_i}. \tag{14}$$

Introducing the following normalization quantities, Eq. (14) can be rewritten as

$$\rho = \rho_c \rho^*, \quad c_p = c_{p_c} c_p^*, \quad k = k_c k^*, \quad T = T_c T^*,$$
$$t = t_c t^*, \quad x_i = l_c x_i^*,$$
$$\rho^* c_p^* \frac{\partial T^*}{\partial t^*} = \frac{\partial\left(k^*(\partial T^*/\partial x_i^*)\right)}{\partial x_i^*}\left(\frac{k_c t_c}{l_c^2 \rho_c c_{p_c}}\right). \tag{15}$$

Hence we obtain the relationship between the time-scale t_c and the wall properties ρ_c, c_{p_c} and k_c:

$$t_c = \frac{l_c^2}{\alpha_c}, \quad \text{where } \alpha_c = \frac{k_c}{c_{p_c}\rho_c}. \tag{16}$$

Defining $\alpha_c^* = (\alpha_c)_w/(\alpha_c)_{air}$, we have $\alpha_c^* = 4.53$ for aluminum, $\alpha_c^* = 0.0164$ for mirror glass and $\alpha_c^* = 0.00504$ for Perspex. Therefore, the heat conduction time-scale ratio $t_c^* = (t_c)_w/(t_c)_{air}$ is about 1:5 for aluminum whereas it is about 61 for mirror glass and about 198 for Perspex. This means, that the temperature conduction in an aluminum wall is about five times as fast as in the fluid, hence the heat feedback from an aluminum wall is very weak, as observed in Fig. 11. On the other hand, in the poorly conducting wall materials such as mirror glass, the temperature conduction is much slower than in the fluid. As a result, the heat feedback from the solid wall is much stronger.

The heat exchange process between the fluid and the solid wall can have a two-way (enhancing and reducing) effect on the heat loss of a wire. Since both highly and poorly conducting materials have $k_w^* \gg 1$, the heat loss from a wire can be enhanced by the heat conduction in

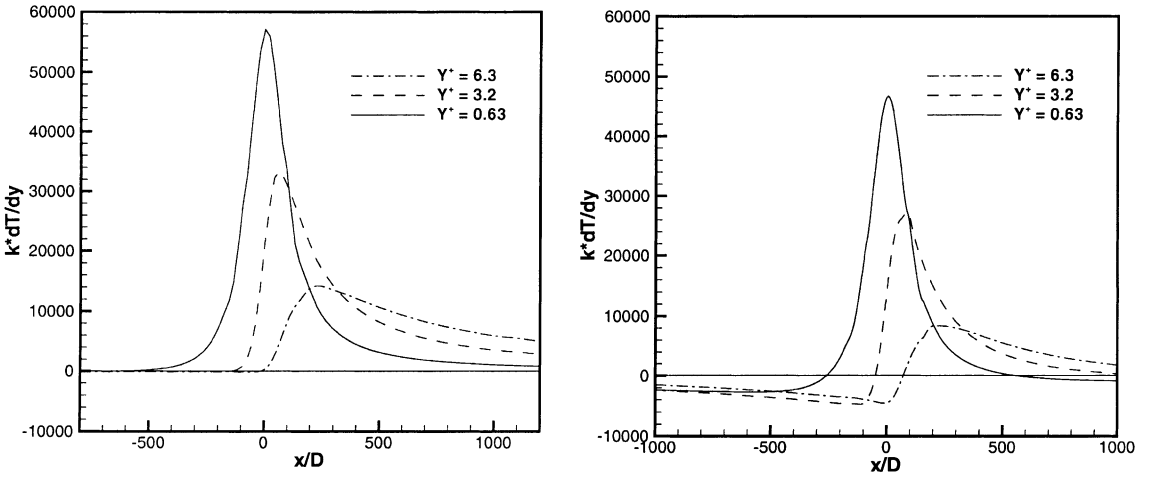

Fig. 11. Heat exchange ($k^*(\partial T/\partial y)$ (°C/m)) at the fluid–wall interface in the cases of an aluminum wall ($k_w^* = 9186$, left) and a mirror glass wall ($k_w^* = 29.6$, right); the heat flux fed back into the fluid is defined as being negative and a positive value means the heat flux from the fluid into the solid wall.

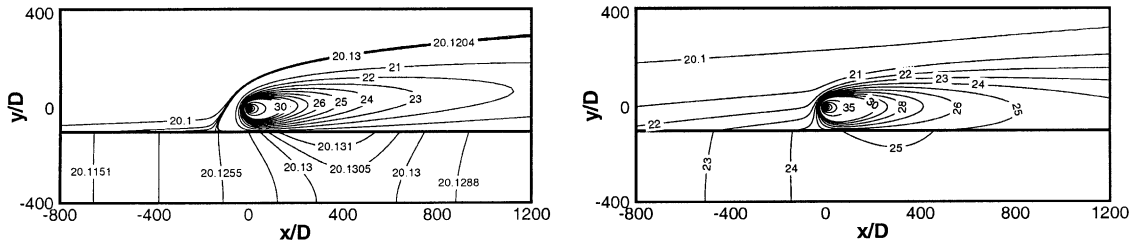

Fig. 12. Temperature isolines (°C) around the cylinder and in the wall at $Y^+ = 3.2$ resulting from $Re_D = 0.1$, $Y/D = 100$. Case (a), an aluminum wall, $k_w^* = 9186$ (left). Case (b), a mirror glass wall, $k_w^* = 29.6$ (right).

the solid wall. However, the heat feedback in the upstream direction from the solid wall can also reduce the heat transfer rate from the wire in the case of poorly conducting walls. This heat feedback is exactly the main physical cause of the negative velocity corrections ($C_U > 1$) predicted in the numerical simulations for poorly conducting wall materials.

Based on the above analysis, the different velocity corrections corresponding to different Y^+ can now be explained both for highly and poorly conducting materials.

When a hot-wire whose temperature is higher than that of the fluid is applied to near-wall measurements, heat transfer from the fluid into the wall material occurs in the interaction region of the "temperature influence region" of the hot-wire and the solid wall. Owing to the heat conduction in the solid wall, part of the heat flux is fed back into the fluid at the fluid–wall interface (both upstream and downstream of the wire location) where the fluid temperature is lower than that in the solid wall. In case (a) in Fig. 10, owing to the strong convection corresponding to a relatively high Re_D or Y^+, the "temperature influence region" is very narrow and the "temperature influence region"–wall interaction occurs far downstream from the wire location. The heat exchange between the fluid and the solid wall has no evident effect on the flow and heat transfer in the core region around the hot-wire. As a result, no velocity correction is required, i.e., $C_U \approx 1.0$, regardless of the wall material. The temperature isolines in Fig. 6 serve as a good example of this case.

In case (b) in Fig. 10, Y^+ decreases to certain range, the contribution of the diffusive heat transfer increases and the "temperature influence region"–wall interaction moves closer to the wire location. The heat transfer from the cylinder is enhanced in the case of an aluminum wall ($k_w^* = 9186$) owing to the increasing heat flux into the solid wall (see the case of $Y^+ = 3.2$ in Fig. 11, left). As a result, a positive velocity correction, i.e., $C_U < 1$, is required. In the case of a mirror glass wall ($k_w^* = 29.6$), the heat flux into the wall is also increased. However, the heat flux fed back into the fluid in the upstream direction from the solid wall is strong in this case (see the case of $Y^+ = 3.2$ in Fig. 11, right), which warms up the oncoming fluid which flows over the region of interest of the wire. As a final result, the "reducing effect" becomes dominant over the "enhancing effect", hence a negative velocity correction, i.e., $C_U > 1$ (region (b) of Fig. 9) is required. For an easier understanding, the field temperature distribution is provided in Fig. 12.

If Y^+ decreases further (see case (c) in Fig. 10), the "temperature influence region"–wall interaction occurs in the proximity of the wire location. Large heat fluxes are transferred into the solid wall owing to the much higher conductivities of the wall materials compared with that of the fluid (see the case of $Y^+ = 0.63$ in Fig. 11), hence the enhancing effect becomes dominant over the reducing effect arising from the heat feedback. Therefore, the heat loss from the wire is significantly enhanced and positive velocity corrections are observed also for poorly conducting materials ($C_U < 1$, region (c) of Fig. 9). For an example of the temperature isolines, see Fig. 5.

5. Conclusions

Accurate numerical simulations were carried out to study the influence of the thermal conductivity of the wall material on the heat transfer characteristics of a cylinder in wall-bounded shear flow. The conjugated heat transfer in the solid wall was taken into account. The effects of the influencing parameters such as the thermal conductivity of the wall material, the cylinder–wall distance, the cylinder Reynolds number and the shear parameter on the local heat transfer rate of a cylinder were analyzed in detail. The coupling process of the heat transfer between the flow region and the solid wall was also analyzed. The present investigation has direct implications for hot-wire near-wall measurements. A better understanding of the physical problem is reached. Based on the present numerical results, the following conclusions can be drawn.

The heat conduction in the solid wall has a significant effect on the heat transfer from a cylinder in a wall-bounded shear flow. The influence range (cylinder–wall

distance) of the wall effect and the intensity at a given distance depend quantitatively on the thermal conductivity of the wall material, especially in cases of poorly conducting walls. When $Y^+ > 5$, the wall effect become negligible for all wall materials.

A "elliptically" shaped local Nusselt number $Nu(x/D)$ distribution was found on the cylinder surface in a shear flow. Beyond the wall influence range, the average Nusselt number and the gradient of the long-axis of the ellipse are principally determined by the cylinder Reynolds number Re_D. The shear effect on the average Nusselt number and the gradient is negligible, but the local distribution of the Nusselt number $Nu(x/D)$ is characterized by the shear parameter G_2^*.

Strong heat feedback was found from poorly conducting walls (e.g., mirror glass, $k_w^* = 29.6$) into the fluid. That can reduce the heat loss rate of the cylinder when it is located at a certain range of distance Y^+ from a poorly conducting wall. As a result, negative velocity corrections ($C_U > 1$) are required for hot-wire near-wall measurements in such cases. The heat feedback from the highly conductive aluminum wall ($k_w^* = 9186$) was very weak in the total range of the cylinder-wall distance Y^+.

The present analysis of the interaction between the "temperature influence region" of a hot-wire and the solid wall and the heat exchange between the fluid and the solid wall has improved the understanding of the physical mechanism for the hot-wire near-wall correction in the cases of different wall materials and under different flow conditions.

Acknowledgements

This work was supported by a fellowship from the German Academic Exchange Program (DAAD) to J.-M. Shi and by a research grant from the Bavarian Consortium for High Performance Scientific Computing (FORTWIHR), which are gratefully acknowledged. The authors also thank Dr. -Ing C. F. Lange (Department of Mechanical Engineering, University of Alberta, Canada) for providing the numerical results for the local Nusselt number of a cylinder in a free uniform flow for comparison.

References

[1] A. Žukauskas, J. Žiugžd, Heat Transfer of a Cylinder in Crossflow, Springer, Oxford, 1985.
[2] T.S. Kwon, H.J. Sung, J.M. Hyun, Experimental investigation of uniform shear flow past a circular cylinder, ASME J. Fluids Eng. 114 (1992) 457–460.
[3] H.J. Sung, M.S. Lyu, M.K. Chung, Local mass transfer from a circular cylinder in a uniform-shear flow, Int. J. Heat Mass Transfer 23 (1991) 143–151.
[4] R.J. Goldstein, J. Karni, The effect of a wall boundary layer on local mass transfer from cylinder in crossflow, ASME J. Heat Transfer 106 (1984) 260–267.
[5] H.H. Bruun, Hot-Wire Anemometry, Oxford University Press, Oxford, 1995.
[6] J.C. Bhatia, F. Durst, J. Jovanovic, Corrections of hot-wire anemometer measurements near wall, J. Fluid Mech. 122 (1982) 411–431.
[7] Y.T. Chew, S.X. Shi, B.C. Khoo, On the numerical near-wall corrections of single hot-wire measurements, Int. J. Heat Fluid Flow 116 (1995) 471–476.
[8] C.F. Lange, F. Durst, M. Breuer, Wall effects on heat losses from hot-wires, Int. J. Heat Fluid Flow 20 (1999) 34–47.
[9] F. Durst, J.-M. Shi, M. Breuer, Numerical prediction of hot-wire corrections near walls, ASME J. Fluids Eng. (in press).
[10] M. Lacroix, A. Joyeux, Coupling of wall conduction with natural convection from heated cylinder in a rectangular enclosure, Int. Commun. Heat Mass Transfer 34 (1996) 59–67.
[11] F. Durst, C.F. Lange, M. Schäfer, Local block refinement using patched grids for the parallel computation of viscous flows, Report LSTM 445/N, LSTM, Universität Erlangen-Nürnberg, Erlangen, 1995.
[12] Verein Deutscher Ingenieure, VDI -Wärmeatlas, sixth ed., VDI, Düsseldorf, 1991.
[13] C.F. Lange, Numerical predictions of heat and momentum transfer from a cylinder in crossflow with implication to hot-wire anemometry, Ph.D. Thesis, Institute of Fluid Mechanics, Friedrich–Alexander University of Erlangen, Nürnberg, 1997.
[14] C.F. Lange, F. Durst, M. Breuer, Momentum and heat transfer from cylinders in laminar flow at $10^{-4} \leqslant Re \leqslant 200$, Int. J. Heat Mass Transfer 41 (1998) 3409–3430.
[15] I. Demirdžić, M. Perić, Finite volume method for prediction of fluid flow in arbitrary shaped domains with moving boundaries, Int. J. Numer. Meth. Fluids 10 (1990) 771–790.
[16] S.V. Patankar, D.B. Spalding, A calculation procedure for heat, mass and momentum transfer in three-dimensional parabolic flows, Int. J. Heat Mass Transfer 15 (1972) 1787–1806.
[17] M. Perić, R. Kessler, G. Scheuerer, Comparison of finite-volume numerical methods with staggered and colocated grids, Comput. Fluids 16 (1998) 389–403.
[18] M. Hortmann, M. Perić, G. Scheuerer, Finite volume multigrid prediction of laminar natural convection: benchmark solutions, Int. J. Numer. Meth. Fluids 11 (1990) 189–207.
[19] C.F. Lange, Personal communication, 2000.
[20] P.M. Ligrani, P. Bradshaw, Subminiature hot-wire sensors: development and use, J. Phys. E 20 (1987) 323–332.
[21] Y.T. Chew, B.C. Khoo, G.L. Li, An investigation of wall effects on hot-wire measurement using a bent sublayer probe, Meas. Sci. Technol. 9 (1998) 67–85.